LEVEL II

3

UNIVERSITY OF CAMBRIDGE
DEPARTMENT OF PHYSICS

REDUCTION OF AERODYNAMIC DRAG

Dr. J.E. FIELD — PRINCIPAL INVESTIGATOR

W.A. WILBY)
W.G. REES) — RESEARCH STUDENTS

Dr. J. CLARK — CONSULTANT

CAVENDISH LABORATORY
UNIVERSITY OF CAMBRIDGE

MAY 1981

INTERIM SCIENTIFIC REPORT No. 2
1 April 1980 - 31 March 1981

Approved for public release

distribution unlimited

Prepared for:

U.S. Air Force Office of Scientific Research (AFOSR)

and

European Office of Aerospace Research and Development
London, England.

Cavendish Laboratory, Madingley Road, Cambridge CB3 OHE.

UNCLASSIFIED (18) AFOSR (19) TR-81-0550

REPORT DOCUMENTATION PAGE	READ INSTRUCTIONS BEFORE COMPLETING FORM
1. Report Number AFOSR-TR-81-0550 ✓ 2. Govt Accession No. AD-A102 064	3. Recipient's Catalog Number
4. Title (and Subtitle) (6) REDUCTION OF AERODYNAMIC DRAG (9)	5. Type of Report & Period Covered INTERIM SCIENTIFIC rept. ~~80 Apr 01 - 81 Mar 31~~
	6. Performing Org. Report Number 1 apr 80 - 31 Mar 81
7. Author(s) (10) J.E. Field, W.A. Wilby, W.G. Rees, J. Clark (15)	8. Contract or Grant Number AFOSR-79-0057 ✓
9. Performing Organization Name and Address Physics and Chemistry of Solids Cavendish Laboratory, University of Cambridge Madingley Road Cambridge CB3 OHE	10. Program Element, Project, Task Area & Work Unit Numbers 61102F (16) 2307 A2 (17)
11. Controlling Office Name and Address Air Force Office of Scientific Research/NA Bolling AFB DC20332	12. Report Date (11) May 81
	13. Number of Pages 47
14. Monitoring Agency Name and Address (12) 48	15. UNCLASSIFIED

16. & 17. Distribution Statement

Approved for public release; distribution unlimited.

18. Supplementary Notes

19. Key Words

AERODYNAMICS DRAG REDUCTION RADIOACTIVITY

BOUNDARY LAYERS TURBULENCE MOLECULAR AERODYNAMICS

20. Abstract

A study is being made of the effect on aerodynamic drag of boundary layer irradiation by radioactive sources. A blow-down wind tunnel and a skin friction drag balance have been designed and constructed. The balance is of the null-position type, and is operated using an automatic control system to maintain the null position of the drag plate. High accuracy and stability are observed at flow velocities up to 200 m/s and resolutions of up to 0.1% of changes in drag have been achieved. In separate experiments, a study of the effect of radioactive emission on gas viscosity is being made with a specially designed torsion disc viscometer. Measurements to date have been at atmospheric pressure with both pieces of apparatus. No significant changes in drag have been found except at low flow speeds. However, future work will be extended to lower pressures where there are reports (ref. 4) of a decrease in viscosity with radiation. An objective of new research will be to find the optimum conditions for any drag reduction. Both forms of apparatus have the sensitivity and flexibility to study aerodynamic drag and gas viscosity for a variety of configurations.

FORM 1473

076550 UNCLASSIFIED

List of Symbols

U_o	Centre line flow velocity
h	Channel height
ρ	density
η	viscosity
$P = \frac{1}{2}\rho U_o^2$	pilot static pressure
D	drag force
V	LVDT voltage
A	plate area
τ	Shear Stress
$Re = \frac{\rho U_o h}{\eta}$	channel Reynolds number
$C_f = \frac{\tau}{\frac{1}{2}\rho U_o^2}$	drag coefficient
v_t	control circuit trigger level
N	no. of weights/swings
n	Sample size
$\bar{x} = \frac{1}{n}\sum x_i$	unbiased estimate of population mean
$\hat{\sigma} = \sqrt{\frac{1}{n-1}\sum (x_i - \bar{x})^2}$	unbiased estimate of population standard deviation
$\hat{\sigma}/\sqrt{n}$	standard error of mean
r^2	regression coefficient (0 - no correlation, 1 - perfect correlation)
θ_n	amplitude of n^{th} torsional oscillation
$\Delta = \ln \theta_n - \ln \theta_{n+1}$	logarithmic decrement

1. INTRODUCTION

A previous report[1] described in detail the development of an aerodynamic skin friction drag balance for drag reduction studies with radioactive irradiation of the air flow. This report describes the continuation of this research. It includes an analysis of possible error sources, improvements in the drag measurement technique, measurements at lower flow speed, the measurement of skin friction drag in both laminar/transitional and fully turbulent flow, and an exhaustive set of measurements on drag reduction by irradiation. In addition, some research using torsion disc viscometry to investigate the effect of irradiation on gas viscosity has been initiated.

In view of the detailed description of the development and construction of the drag balance given in the previous report, only a brief resumé of its salient features will be given in this report, which will concentrate on the experimental data obtained with the balance.

The torsion disc work is at an early stage. An account is given of the design and construction of a prototype torsion disc viscometer, together with an analysis of the data obtained so far.

2. DRAG BALANCE EXPERIMENTS

The drag balance is of the floating element type and is usually operated in the null position mode, the drag force being balanced by coils and magnets acting so as to keep the drag element in the null position. The displacement is measured very accurately using a linear variable differential transformer (LVDT), (See Figs. 1 and 2). The balance can also be operated in the deflection mode. This is done for very small forces (< 300 mg force), the drag being determined from the LVDT voltage corresponding to the deflection of the drag element against its resilient piano wire suspension.

The centre line flow velocity at the windtunnel test section is determined using a miniature pitot tube and static orifice just downstream of the drag element. The pressure is measured on a precision dial manometer for pitot static

pressures greater than 1 mmHg. For lower pressures a tilt paraffin manometer is used. The static pressure in the balance housing is also monitored with a paraffin manometer as a check for leaks which would affect the drag readings. The air temperature in the housing is monitored by thermocouples.

In the null position mode, the null position is maintained by an automatic control circuit. This is triggered by the displacement of the plate as measured by the LVDT. The coil current necessary to maintain the null position is measured i terms of the voltage across a 2.7 Ω resistor in series with the coils. This voltage is fed to a DVM and to an X-Y recorder. The true drag voltage can be most easily determined from the fluctuating voltage (due to vibration and fluctuating flow speed) by looking at a trace on the recorder for a period of 5 seconds or so. This method has advantages over an integrating circuit and voltmeter, as the response of the drag balance to a vibration of moderate amplitude is easily recognisable, and can be ignored, whereas the integral of a damped simple harmonic vibration would be non zero. For deflection measurements at low speed and high sensitivity, an integrating circuit has to be used to eliminate low frequency hum and to protect against large amplitude vibrations. Fig. 3 shows a block diagram of the windtunnel instrumentation.

In order to make drag measurements in fully turbulent flow a 0.91 mm dia. (20 SWG copper wire) boundary layer "trip" can be placed against the upper windtunnel surface at a point 110 mm upstream of the leading edge of the drag plate. This gives fully turbulent flow down to the critical channel Reynolds number.

2.1 Summary of Previous Research

The previous work showed that the drag balance and control circuit worked well, and that it was possible to measure drag forces with good accuracy and consistency. However, some problems were experienced with the construction and mounting of the radioactive plates in the drag balance.

Some tentative results were obtained which showed a drag reduction, but the accuracy was poor and it was not possible to make an extended series of readings.

2.2. Analysis of Error Sources

As mentioned in the previous report, it is not necessary to obtain an absolute determination of the drag coefficient. This is because systematic errors due to factors such as plate misalignment or pressure gradients only result in a reduction of the sensitivity of the drag reduction measurements. For example, a spurious contribution of 10% in the drag force would reduce a 1% resolution in drag change to 1.1%. However, the magnitude of some of these effects was investigated to ensure that they were of a low enough order.

Of primary importance, though, is the degree of consistency between measurements with different active plates mounted in the drag balance. Due to the imperfections of the surfaces of the plates, and the difficulty of getting a sufficiently accurate alignment with the lower windtunnel surface, the drag measurements were not adequately reproducible. It was decided to instead have the radioactive foils not in contact with the flow, but to fix a 1/16" perspex (PMMA) shield in the lower wall of the windtunnel. This gives a 20% reduction in the radiation level near the drag element for the ^{147}Pm sources, emitting 0.22 MeV β particles. This is more than compensated for by the improved accuracy of measurement. The α source (^{210}Po) cannot, of course, be used in this configuration; the γ(^{58}Co) source can, but these experiments have not yet been performed. As the sources are no longer in contact with the flow, the exhaust duct is not needed, permitting more frequent calibration.

As mentioned at the start of this section, measurements have been made at lower flow speeds. For low speed null position measurements, the LVDT deflection voltage is comparable with the trigger levels of the control circuit.

It was thought that this might lead to inaccuracies, but in fact trigger levels of two or three times the standard did not significantly degrade the performance of the control circuit. At medium speeds (Fig. 4) the difference observed is of the order of the consistency of the drag measurement.

To evaluate the effect of the pressure difference on the ends of the drag element, a special drag plate was constructed with ½ mm dia. static taps in the ends, at 1½ and 3 mm from the surface of the plate, connecting with small capillary paraffin manometers suspended with the drag element. These registered pressure differences of as little as 0.02 mmHg.

Measurements made over a range of flow velocities show that the effect of the pressure gradient is by no means simple, in fact, there can even be a pressure force acting upstream (see Fig. 5; a +ve difference corresponds to a downstream force, -ve an upstream force). This force is also influenced by the orientation of the plate, i.e. the up and downstream gapsize, and more strongly, by the alignment with the windtunnel wall (see Fig. 6. Data are for the static tap at 1.5 mm).

Fig. 7 shows the typical % contribution of the pressure force to the total force. The calibration of the manometers had to be estimated, and may be rather inaccurate. Several measurements taken at positions of zero pressure difference show that the basic character of the drag curve is unaffected by the pressure force However, as in the recent series of experiments the radioactive plates were mounted in the lower windtunnel wall, and not as a drag element, it was possible to redesign the drag element with the ends cut at 45° to a sharp edge. This, of course, reduces the effect of the pressure gradient, although the system is possibly more sensitive to misalignment.

2.3 Experimental Results

Before beginning measurements with the radioactive sources, a comprehensive set of drag measurements was taken to check the performance of the system. Fig. 8 shows a typical calibration curve for the balance in the deflection mode; fig. 9 a calibration curve for the null position

shown in Fig. 10.

It can be seen that with the boundary layer trip in place the flow becomes turbulent above a channel Reynolds number of about 2500 and is essentially fully developed by about Re = 4000. Without the trip the flow remained laminar up to Re = 9000, when transition to fully turbulent flow beings. Although transition seems complete by Re = 30,000 it can be seen that the drag coefficient is still less than before. This is probably due the turbulence being initiated at a different position along the windtunnel. The data are in good agreement with ref. 2 and 3.

Measurements with radioactive sources were then made in the null position mode. The measurements are presented in Tables 1 and 2. * denotes a measurement which has been estimated for computational purposes as the original reading was either missing or more than 3 standard deviations from the mean. Plates N1 to N5 are inactive; A1 and A2 contain approximately 100 and 50 mCi of ^{147}Pm respectively.

The measurements have been corrected to 20°C by using a least squares regression on the balance housing temperature to determine the temperature coefficient for the measurements (See Figs. 11 and 12).

This incorporates the temperature dependence of the calibrations, which otherwise showed no significant systematic errors.

The mean and standard errors($\hat{\sigma}/\sqrt{n}$) of the temperature corrected measurements are given in Tables 3 and 4. "N" and "A" denote null and active measurements combined.

Tables 5 and 6 give the % drag changes observed. The errors have been calculated from the standard errors combined in quadrature and expressed as a percentage of the null measurement.

It can be seen that the accuracy of these measurements is much better than the preliminary data of ref. 1, and in fact at high flow speeds, the original estimate of $\pm$ ½% resolution in drag change has been bettered to $\pm$ 1/10% (ca. 5 mg in drag force).

Fig. 13 shows the null measurements in the form D/P ($\propto C_f$) vs $\sqrt{P}$ ($\propto$ Re), showing the structure of the flow at each of the pitot static pressures. If the values of the drag coefficient and Reynolds number are required explicitly, comparison can be made with Fig. 10 . The data from the first report are also shown; the curve is displaced as the calibration is different.

Another series of measurements at very low flow speeds, using the deflection mode, was recently initiated, but unfortunately has not been completed due to equipment malfunctions. It is hoped to finish this work soon, so as to provide measurements of drag changes over as wide a range of Reynolds numbers as possible, and to improve the accuracy of the P = 2 and 5 mmHg results.

3. TORSION DISC VISCOMETER

3.1 Review of Work by Kestin and Shah

Kestin and Shah[4] made an experimental investigation of changes in the apparent viscosity of gases produced by ionization. They used a torsion disc viscometer to measure the apparent viscosity, and radioactive sources to produce ionization of the gas within the viscometer. Two approaches were used:

1. a ^{137}Cs Source (ß-emitter) external to the disc.
2. a ^{210}Po Source (α-emitter) contained within the disc.

Measurements were made on the following gases at room temperature and at pressures ranging from 1 to 1300 mmHg (10^{-3} to 1.3 atm.): Air nitrogen carbon dioxide, oxygen, helium, neon, argon, krypton and xenon.

Kestin and Shah used an oscillating (torsion) disc viscometer principally because of the simplicity of design, and also because the results obtained are precise. They were interested to determine the absolute viscosities as well as the fractional changes induced by ionization, and so they had to make elaborate calculations to obtain the former from the measured quantity (the logarithmic decrement, or damping, of torsional oscillation). The dimensions of their apparatus were such that the discs were of 3 to 4 cm diameter.

The results obtained by Kestin and Shah may be summarised thus:

1) External source 97.5 Curie - changes in apparent viscosity at 1 atmosphere, no significant change (< 0.05%) except Kr (+ 0.22%), Xe (+0.14%) and air (- 0.25%).

2) Internal source ca. 0.5 Curie at 1 atmosphere, mostly detect significant (>0.5%) changesin the range - 1% to + 3% at 1 mmHg, usually increases of 1% to 2% except for a significant descrease of 7.6% in the case of air.

3.2. Introduction to the Present Torsion Disc Viscometer Work

It was decided to use a torsion disc viscometer, again for reasons of ease of construction and of precision. Since we did not require to know the absolute viscosity, it was assumed that the logarithmic decrement Δ would be nearly enough proportional to the viscosity over the likely range of variation. This greatly simplified the calculation. The theory of this form of viscometer is outlined in section 3.3 - 3.4.

The work described here represents principally the investigation of a suitable design for a viscometer, with a number of preliminary results for atmospheric air at room temperature, the disc being irradiated externally by β or α radiation.

3.3. Prototype Design

The body of the prototype viscometer was made from dural. The disc itself was of stainless steel. The torsion wire was held by two pinchucks, one fixed in the torsion head and one in a brass clamp which could be screwed down onto the disc. In this way both the wire and the disc could be changed. The brass clamp was fitted with a small plane mirror (aluminized glass). The viscometer was fitted with two 'perspex' windows, to allow the passage of a laser beam (He/Ne) to and from the mirror; this beam was reflected onto a screen, calibrated in millimetres, about two metres distant. The base of the

viscometer , which gave access to the disc, was a push fit and, like the torsion head, sealed with a rubber 'O' ring (Wilson seal). The initial design of the viscometer is shown in Figs. 14-16.

Preliminary experiments were performed using various torsion wires and a disc of diameter 63.5 mm and thickness 0.8 mm (nom.) Torsional oscillations were started by slowly twisting the torsion head and then returning it to its original position, as nearly as possible. The procedure was found to require care in order not to induce too much vibration in the suspension; even so, it was usually necessary to wait about 10 minutes for the grosser perturbations to die away. The logarithmic decrement Δ was measured by converting the amplitudes of about 50 swings of the tight-spot on the screen into the angular amplitude of oscillations of the disc. A graph (Fig 17) shows typical results. The results of the preliminary experiments are given in Table 7.

At this stage some modifications were made. It was thought advisable to have a means of levelling the viscometer accurately. The disc itself was used as a plumb-line. A 'perspex' insert 2 cm long was put into the shaft of the viscometer. The external section of this insert was square, with a thin vertical line scratched and inked, centrally on each face. The viscometer was stood on a levelling plate, which was adjusted until the torsion wire was coplanar with each of the two pairs of opposite lines.

The viscometer was next fitted with a gas port - a short length of pipe sealed and welded to the upper surface of the body. It was connected to a manometer and partially evacuated: in this way it was possible to locate and seal any leaks with "Araldite".

In order to reduce the labour involved in calculating Δ from the data a computer program was written, and several experiments were performed to find how accurately and how reproducibly Δ could be measured. Preliminary attempts were made to find the effect on Δ of placing radioactive plates, containing ^{147}Pm (a β emitter) at an activity of about 150 mCi on the base

of the viscometer, and then comparing the results with those from "dummy" (inactive) plates. This involved removing the base from the viscometer between experiments, which was unsatisfactory, since it disturbed the torsion wire. Experiments were also tried with the base removed and the viscometer positioned above the radioactive plates. The results obtained are contained in Table. 8.

It was found that the values of Δ recorded in these experiments varied by about 6%. The reason for this was not known, but it was conjectured that it was due to vibration. In an attempt to reduce the effect a heavier disc (3.2 mm (nom.) thickness) was used, and a stand was designed to isolate the viscometer from vibration and to aid temperature control. Finally the base of the stand was made a screw fit so that it could be removed and replaced with the minimum of disturbance (Fig. 18).

Further experiments were performed with the heavier disc, using 38 gauge (0.15 mm) Cu/Be wire. The reproducibility was a little better than before. An encapsulated source of ^{58}Co (γ emitter; about 0.3 mCi) was compared with a dummy cut from dural. A thermocouple was led through the gas port in order to assess any correlation between Δ and temperature. Also, experiments were performed on the computer to asses the effect on the measured value of Δ of misreading the zero position on the scale or of incorrectly measuring the distance from the viscometer to the scale. These experiments were made by using one set of data, and varying these parameters each time they were put through the computer. The results of these experiments are contained in Table 9 and 10. A significant correlation was found between Δ and temperature and this is shown in Fig. 19 and corrected for in the final results.

3.4 Theory of the Torsion-Disc Viscometer

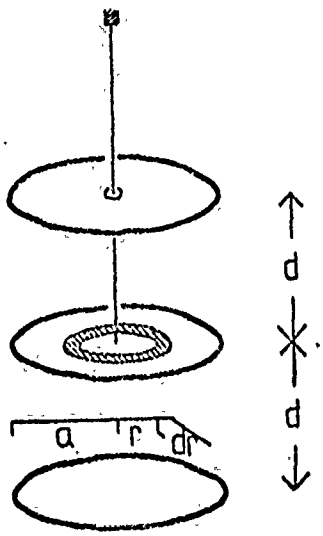

A disc of radius a experiences a couple $-\mu\theta$ when it is twisted through an angle θ in its own plane, about its centre. It lies between two parallel, fixed discs each at a distance d. Suppose this disc has an angular velocity ω and consider the force acting on the element of one surface lying between circles of radii r and r + dr.

Velocity at surface of disc = ωr

velocity at fixed disc = 0 (no-slip conditions)

$\therefore$ velocity gradient = $\frac{\omega r}{d}$

$$\therefore \quad dF = \eta \cdot \frac{\omega r}{d} \cdot 2\pi r dr$$

Thus the torque acting on the element is

$$dG = \frac{2\pi\eta}{d} r^3 dr$$

and the total torque acting on both sides of the disc is $\frac{\pi\eta a^4}{d}$

Thus we can write the equation of motion of the disc:

$$I\ddot{\theta} + \frac{\pi\eta a^4}{d}\dot{\theta} + \mu\theta = 0$$

where I is the moment of inertia. The solution is a dampled simple harmonic motion

$$\theta = \theta_0 e^{-\alpha t}\sin(\omega t + \phi) \quad \text{(for light damping)}$$

where

$$\omega = \left(\frac{\mu}{I}\right)^{\frac{1}{2}}$$

and

$$\alpha = \frac{\pi\eta a^4}{2Id}$$

$$\Delta = 2\pi\alpha/\omega$$

$$= \frac{\pi^2 \alpha^4}{d} (I\mu)^{-\frac{1}{2}} . \eta .$$

In other words Δ is proportional to η. In practice, the damping term is of the form $\left(\frac{\pi\eta a^4}{d}+k\right)\dot{\theta}$, and so $= c\eta + \Delta_o$, but the term Δ_o (arising from mechanical defects in the wire, and so on) is sually very small (typically 5×10^{-5}).

More importantly, "edge effects" should be taken into account, which depend upon the finite thickness of the disc. However, these merely have the effect of altering the calibration of the instrument with the viscosity and density of the gas contained, and since these change by the order of 1%, this is an error in the measured change of viscosity which will be due to edge effects. On the other hand, if an absolute measure of viscosity is requir it will be necessary to produce empirical claibration curves.

4. SUMMARY OF EXPERIMENTAL RESULTS

The results of the drag balance measurements are summarised in Figs. 20 an 21. It can be seen that for both sets of measurements the drag changes for P $\geq$10mmHg (ca. 50 m/s) are entirely consistent with no change in drag force on irradiation, and that any change for the higher flow velocities is less than ca. 0.2%. For P = 2 mmHg there is an apparent drag reduction of a few %, most significant for the turbulent flow. This measurement is still, however, less than 2 standard deviations from no change. The increase for P = 5 mmHg (laminar flow) in conjunction with the P = 2 mmHg decrease could be taken as evidence for a change in the structure of the developing turbulent flow (see Fig. 13).

The torsion disc measurement with the ^{147}Pm plates gave a change of viscosity of + 0.08 $\pm$ 0.26% while for ^{58}Co the change was 0.0 $\pm$ 1.2%, both consist with no change.

5. DISCUSSION AND CONCLUSION

As this report describes, we have now completed the construction and evaluation of a drag balance and a torsion disc viscometer. Both are instruments of high precision which allow us to study changes of drag and viscosity in gases to high accuracies. To date they have been used to investigate any changes caused by radioactive irradiation at atmospheric pressure.

Both the theoretical and experimental work of Kestin and Shah[4] suggest that only a very small drag change is to be expected at atmospheric pressure with the radiation intensities used. This is in agreement with calculations using the Chapman Enskog theory (see Ref. 5) which suggests that the size of the drag (or viscosity) change is of the order of the ionisation intensity. The present experimental work seems to be in agreement with these results, although there is a possibility of an anomalous drag reduction at low flow speeds.

We now plan to extend our research to lower speed measurements and also to begin work at pressures less than atmospheric. These experiments should prove exciting since there is evidence of a viscosity decrease for air, caused by radioactive bombardment at lower pressures (ref. 4). The research will be directed at finding the optimum conditions for any decrease of drag.

Experiments are also planned to establish the basic mechanisms involved in any drag reduction. The three possibilities which will be examined initially are that it is due to (i) ionization (ii) thermal input at a critical part of the boundary layer (iii) molecular clustering. The apparatus described in this report has the flexibility to test these various possible mechanisms and with techniques already available in the laboratory, such as high-speed photography, flow visualization and mass spectrometry, it should be possible to make a full investigation of drag reduction processes.

REFERENCES

1. J. Clark, J.E. Field and W.A. Wilby, Reduction of Aerodynamic Drag, Interim Scientific Report No. 1. May, 1980.

2. H. Schlicting, Boundary Layer Theory. McGraw-Hill, 1959 (7th ed.)

3. V.C. Patel and M.R. Head, Some Observations of Skin Friction and Velocity Profiles in Fully Developed Pipe and Channel Flows. J. Fluid Mech. 38 (1969).

4. J. Kestin and V.L. Shah, Effect of Long Range Intermolecular Forces on the Drag of an Oscillating Disk and on the Viscosity of Gases. AFFDL-TR-68-86.

5. Hirschfelder, Curtiss and Bird, Molecular Theory of Gases and Liquids. Wiley, 1967.

Figure 1 WINDTUNNEL SYSTEM

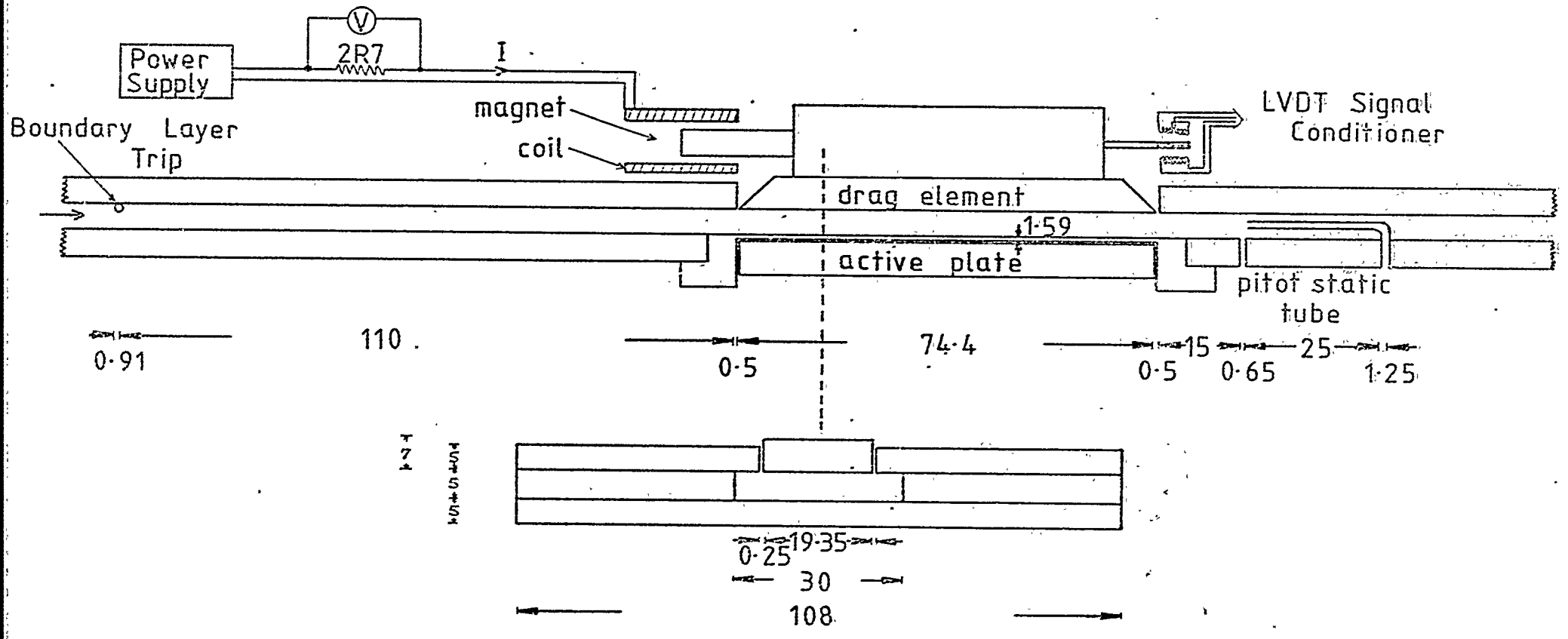

Figure 2. Diagram of Windtunnel Test Section.

Dimensions in mm. Details of Suspension and Housing Not Shown.

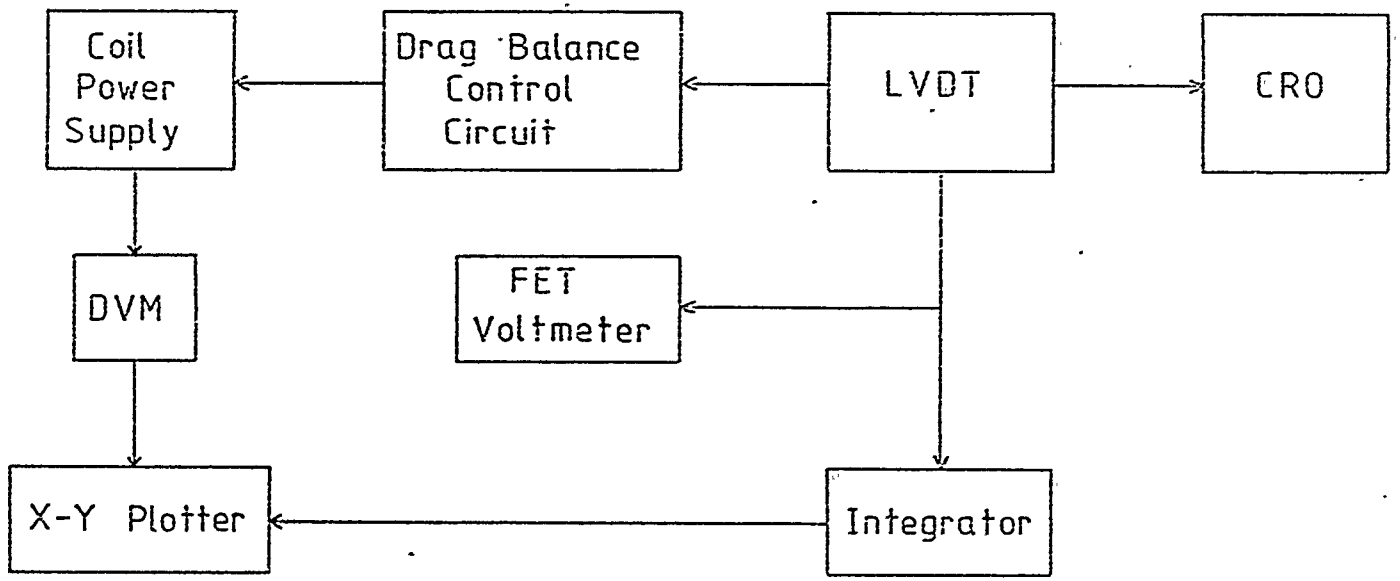

Figure 3. Block Diagram of Instrumentation.

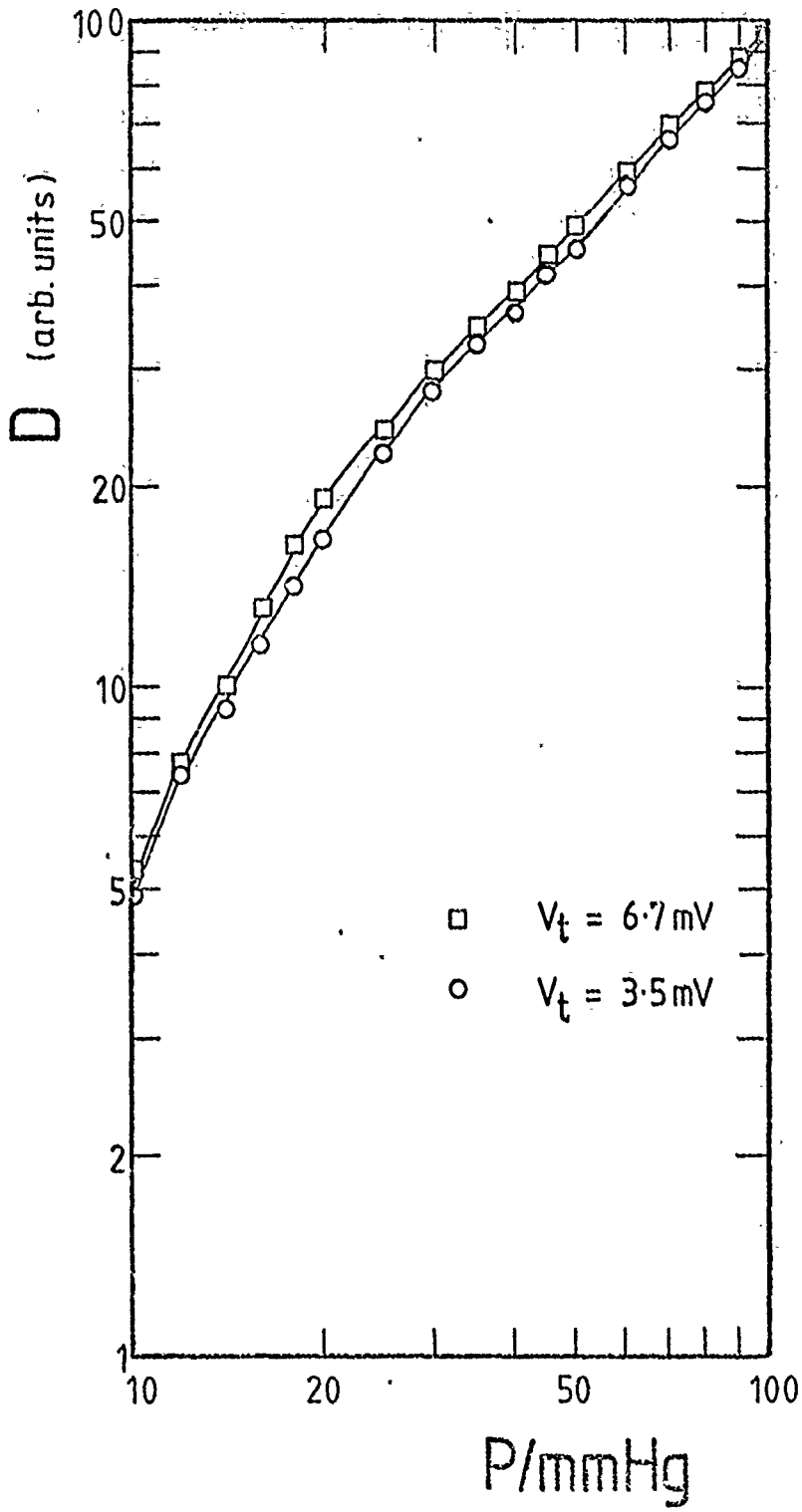

Figure 4. Effect of Control Circuit Trigger Level.

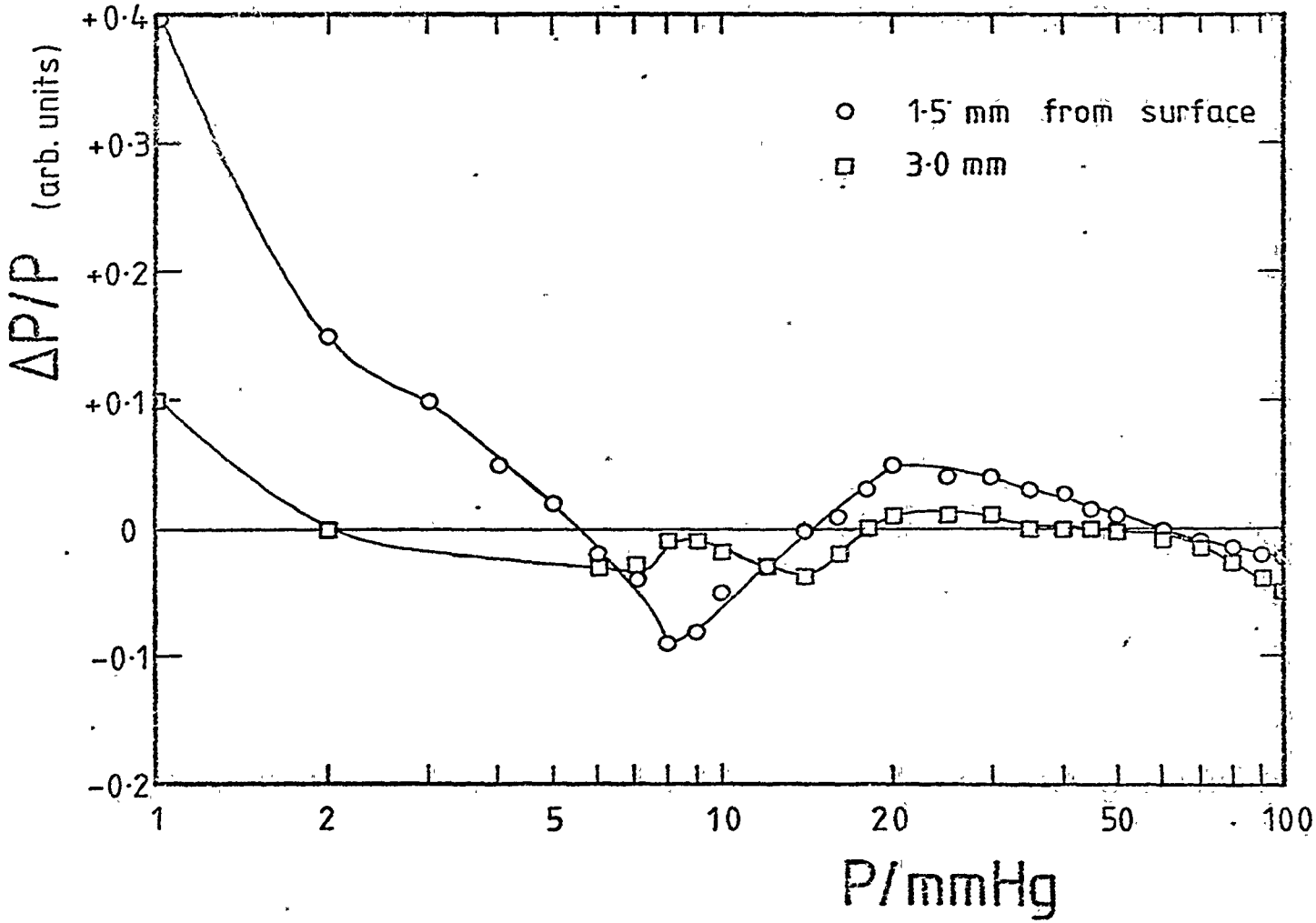

Figure 5. Reduced Pressure Difference on Drag Element.

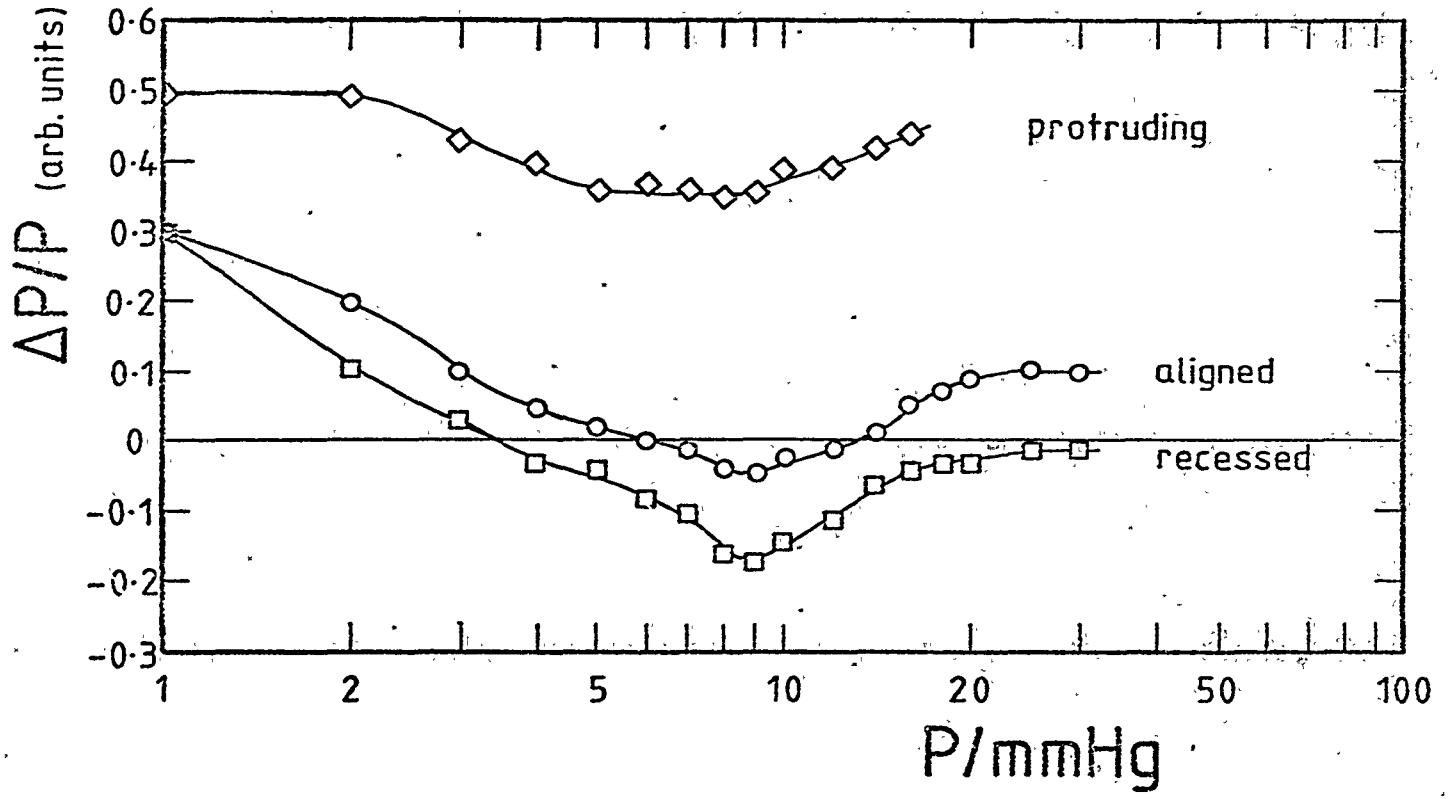

Figure 6. Effect of Plate Alignment on Pressure Difference.

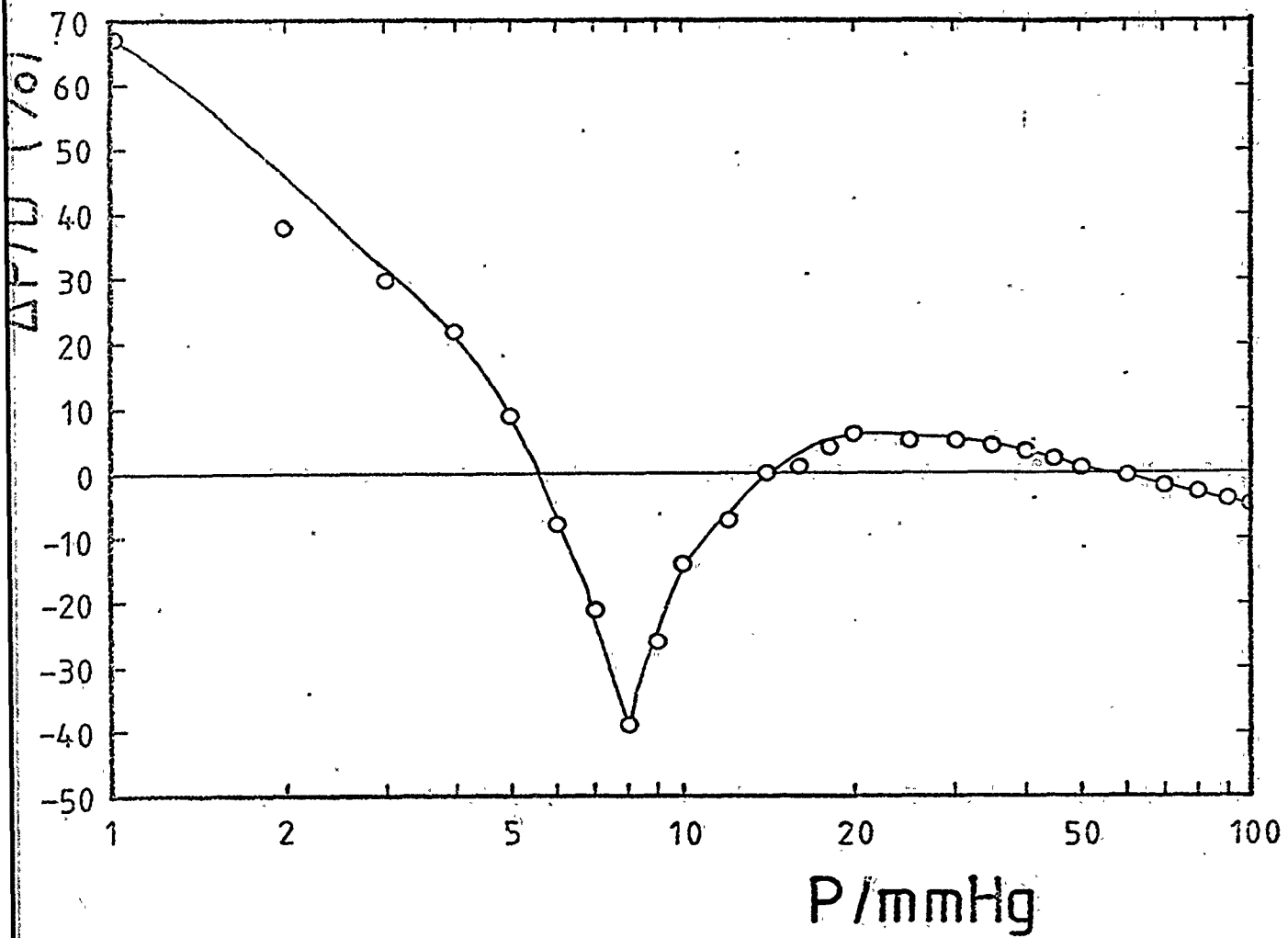

Figure 7. Contribution of Pressure Force.

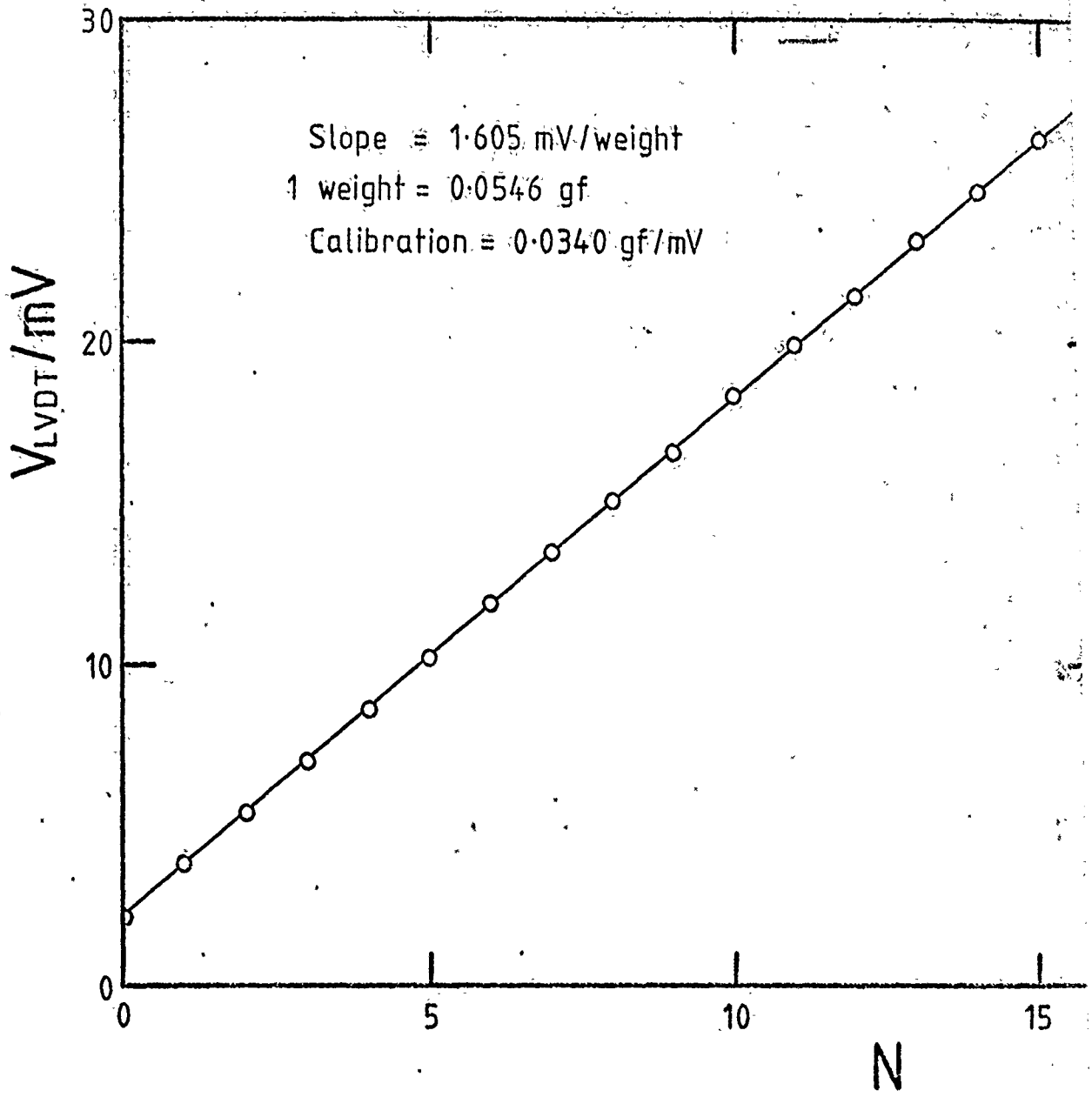

Figure 8. Typical Calibration Curve (deflection mode).

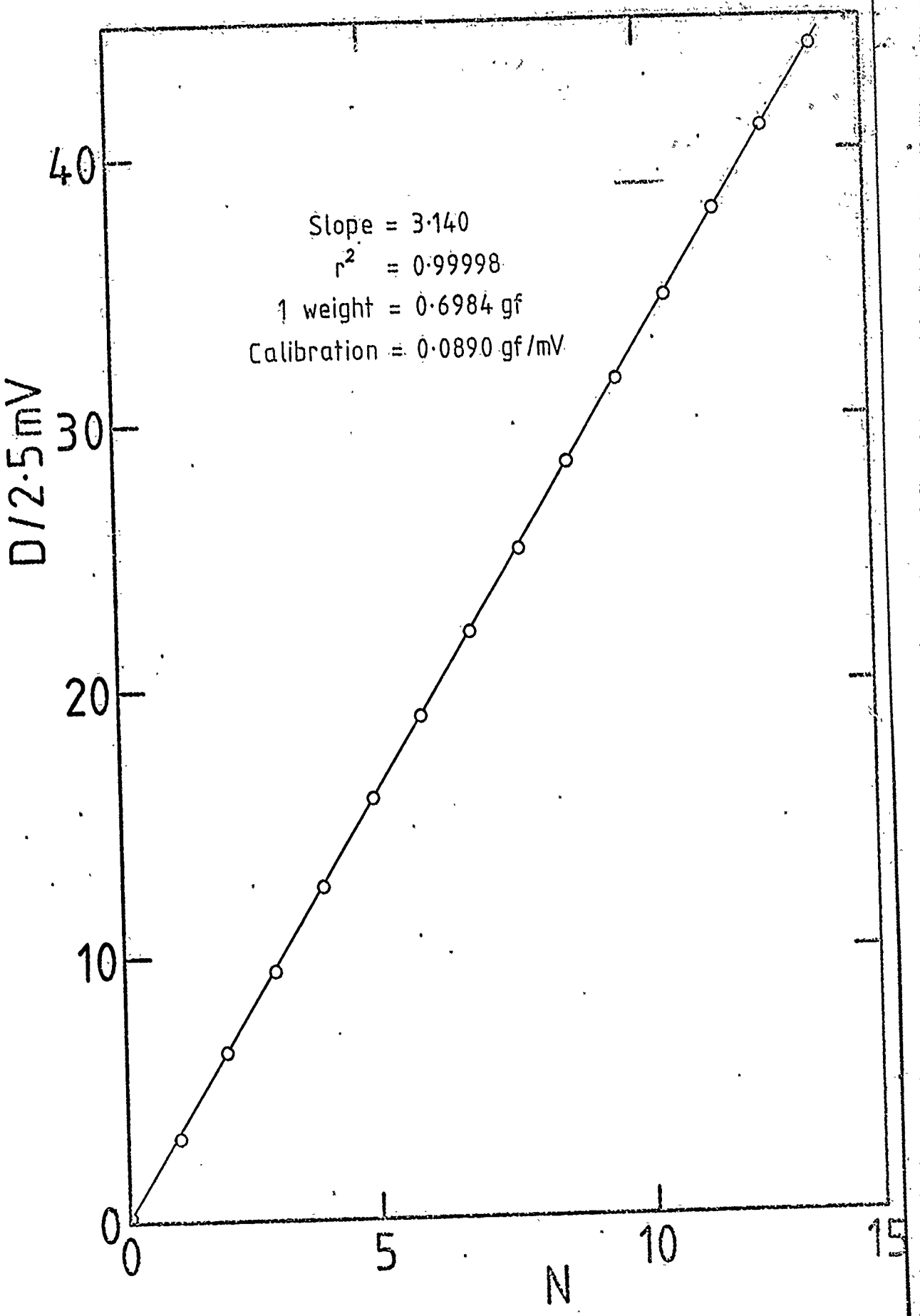

Figure 9. Typical Calibration Curve (null position mode).

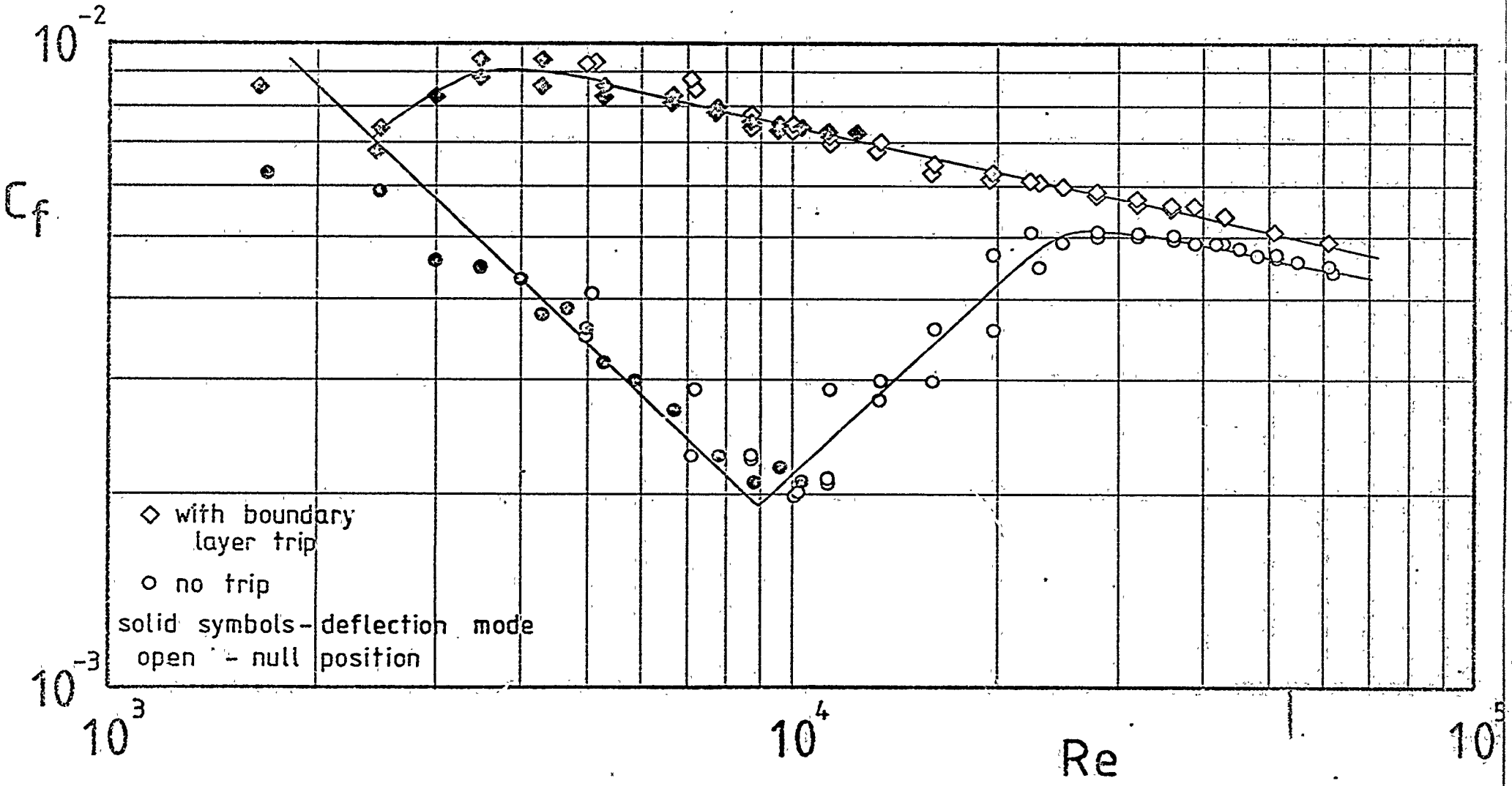

Figure 10. Drag Coefficient vs Reynolds Number.

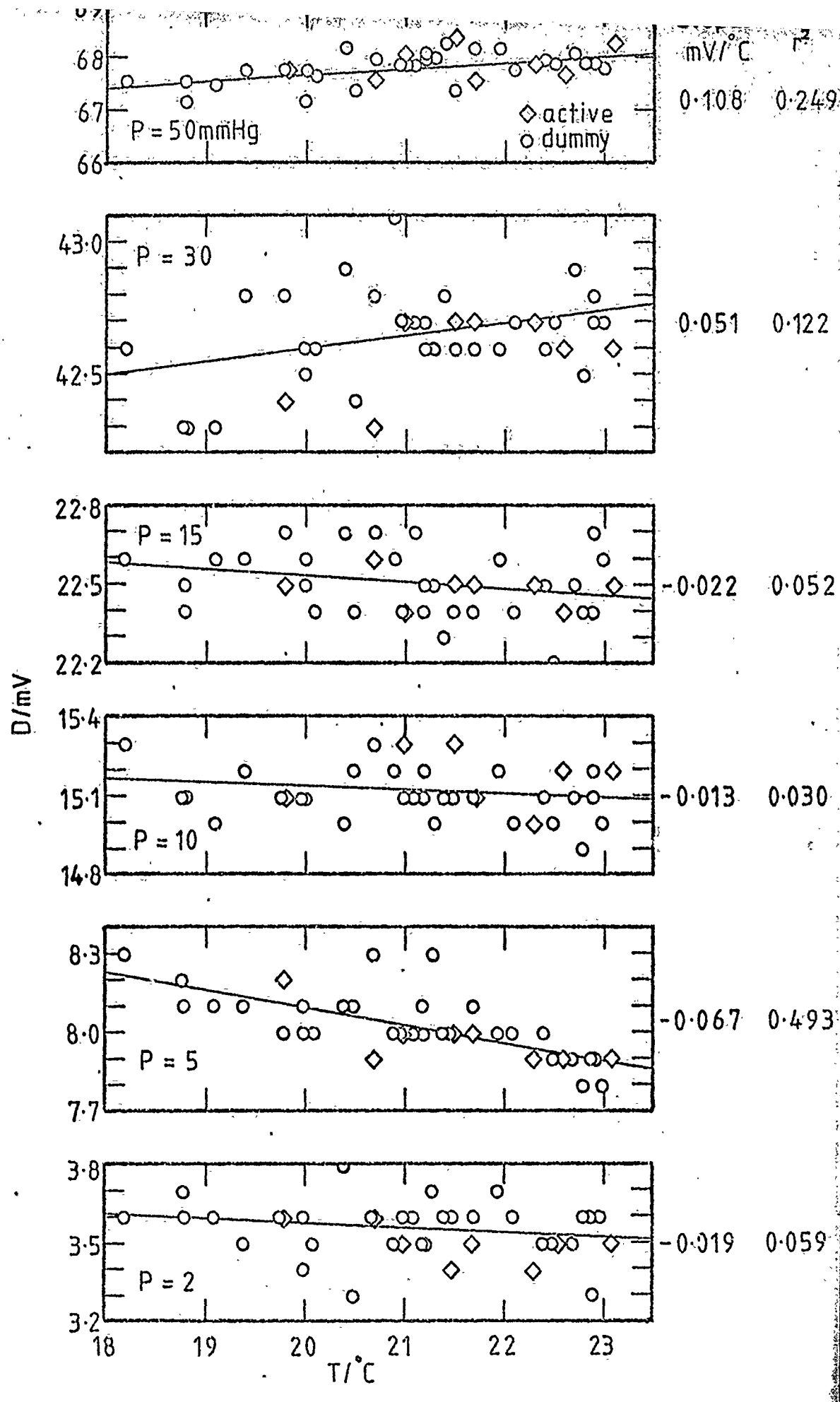

Figure 11. Temperature Dependence of Drag Measurements (fully turbulent).

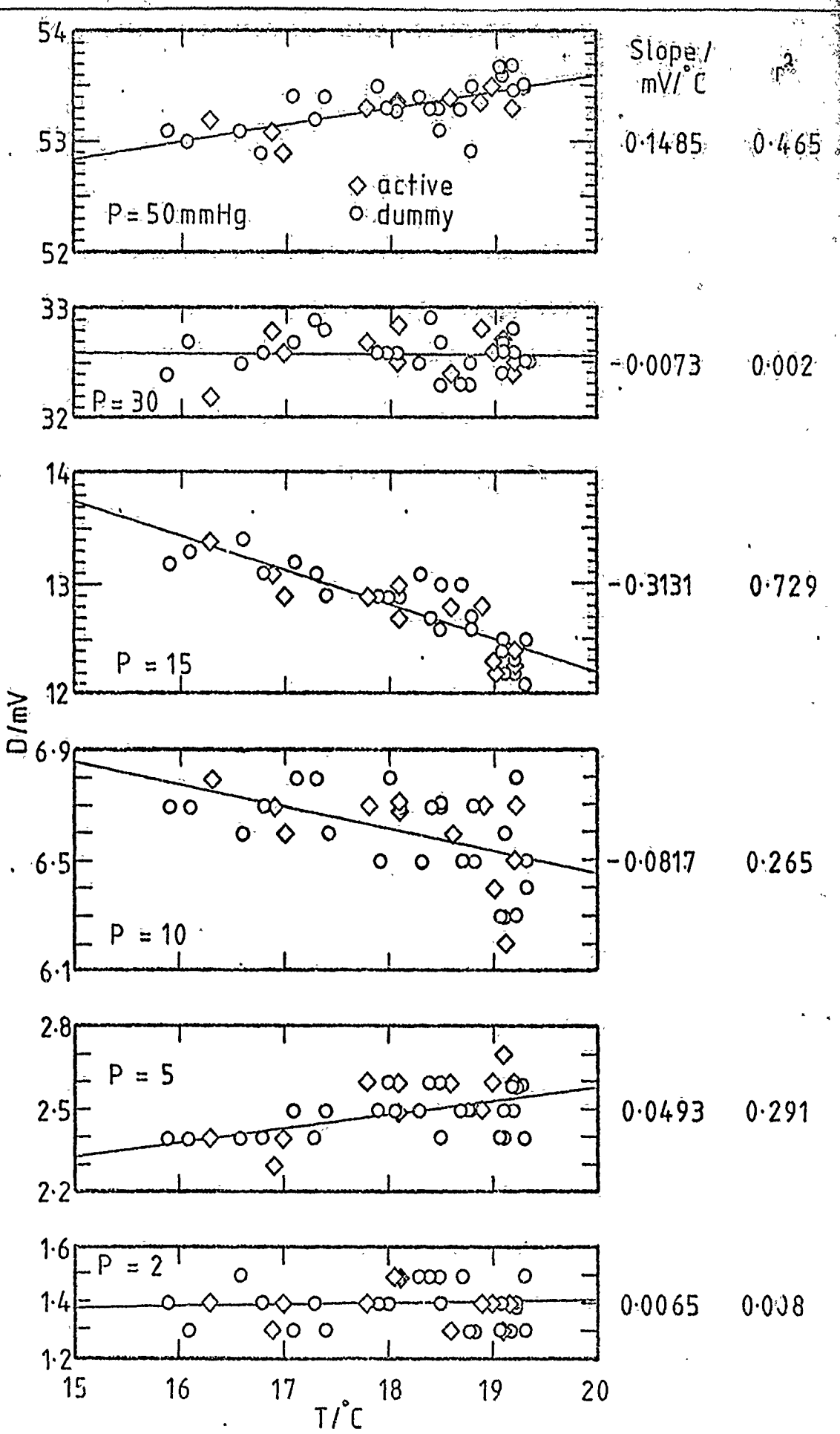

Figure 12. Temperature Dependendence of Drag

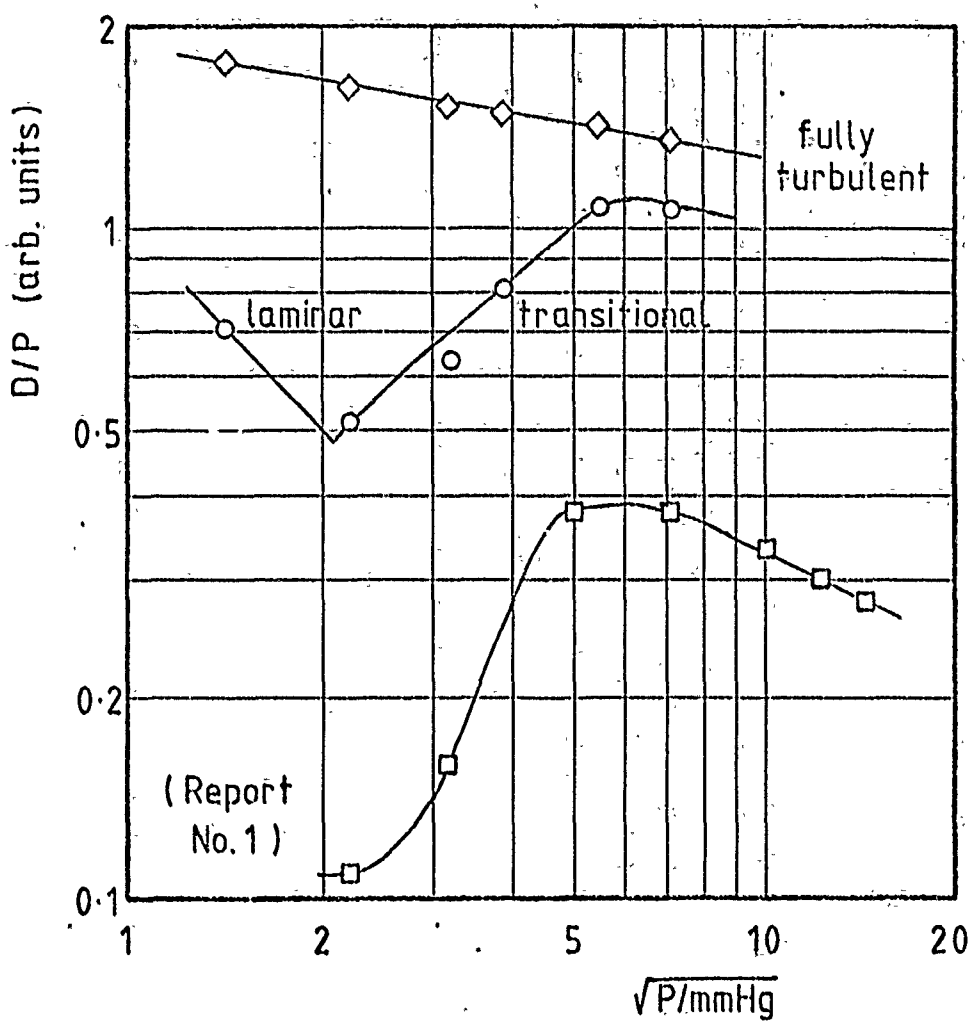

Figure 13. Drag Coefficient vs Reynolds Number.

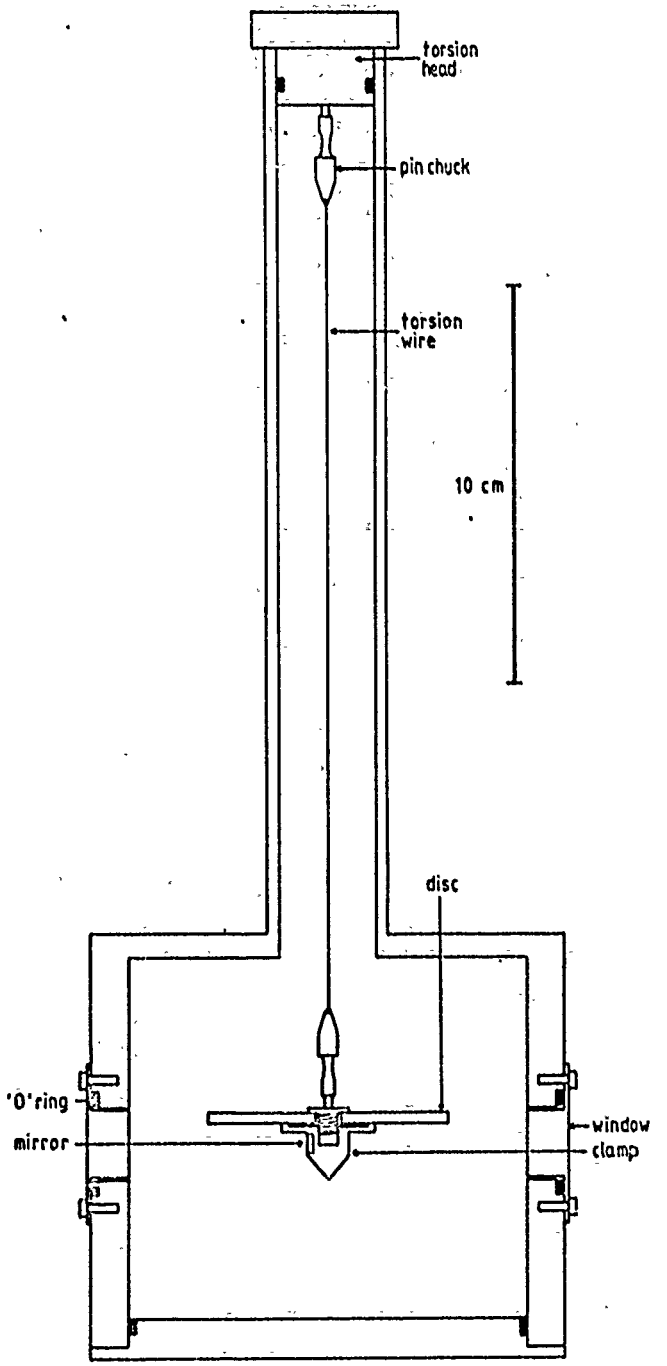

Figure 14. Prototype torsion disc viscometer.

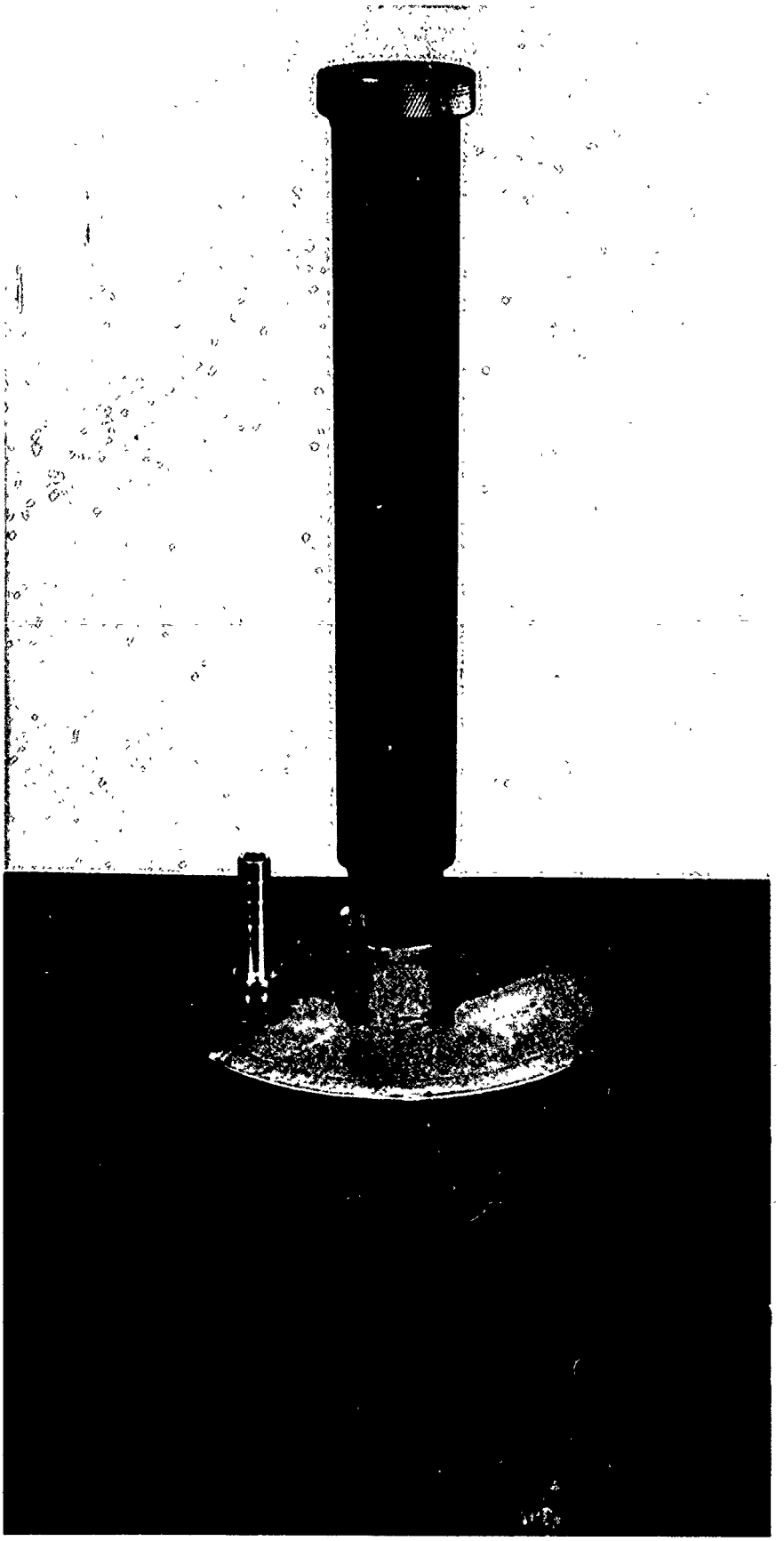

VISCOMETER
Figure 15

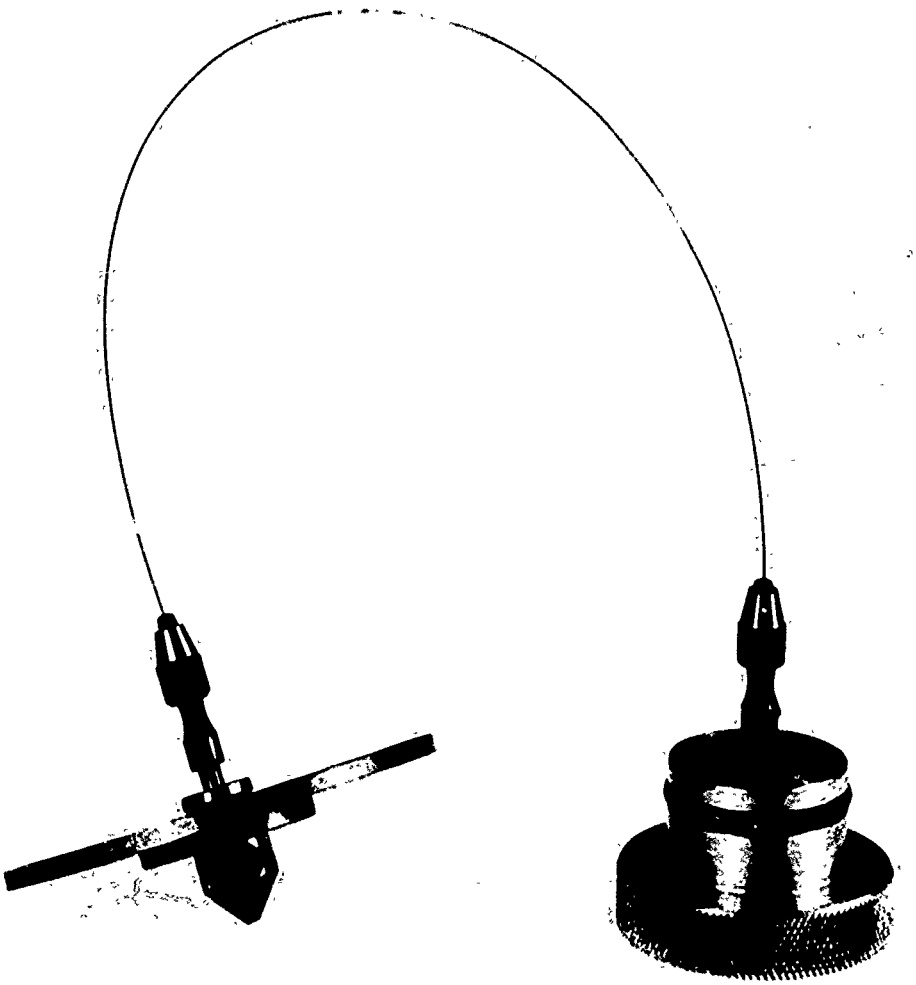

TORSION DISC
Figure 16

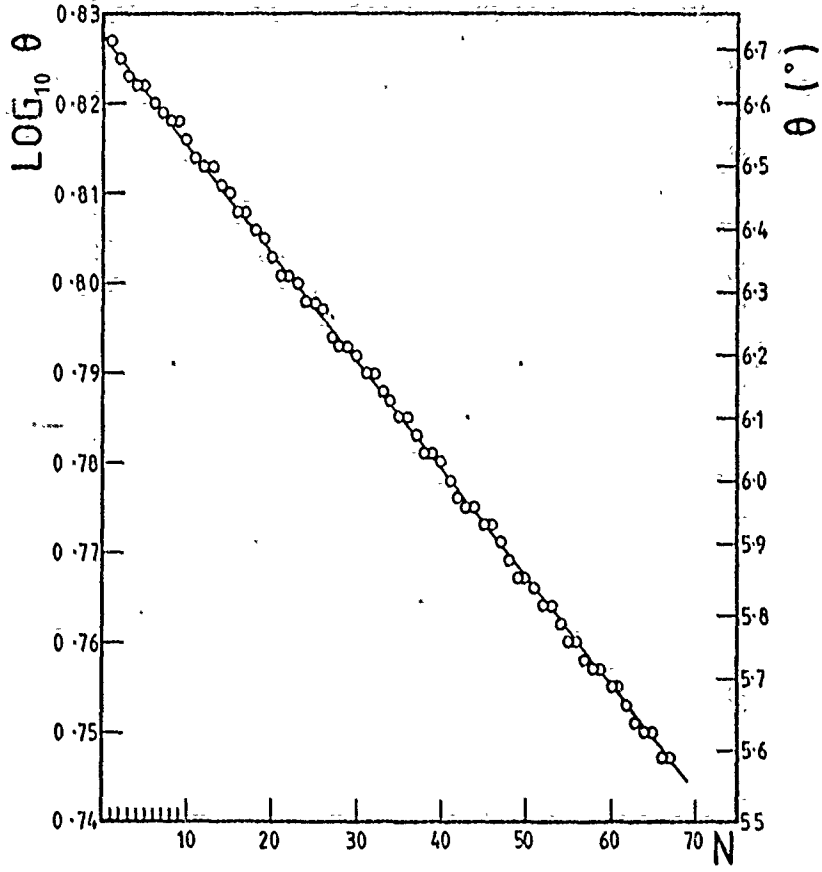

Figure 17. Amplitude of disc oscillation (θ) plotted against number of swing (N).

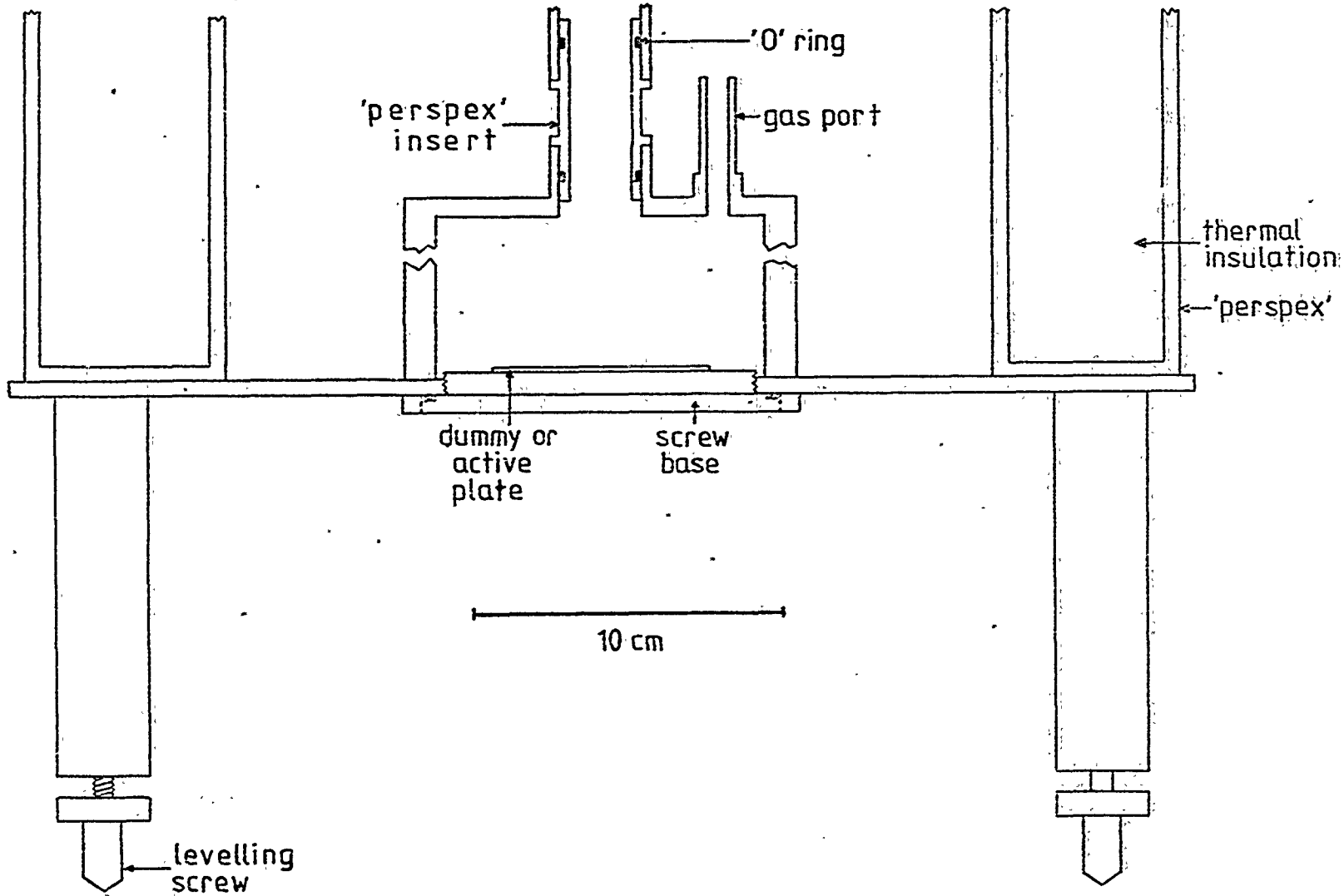

Figure 18. Modifications to viscometer.

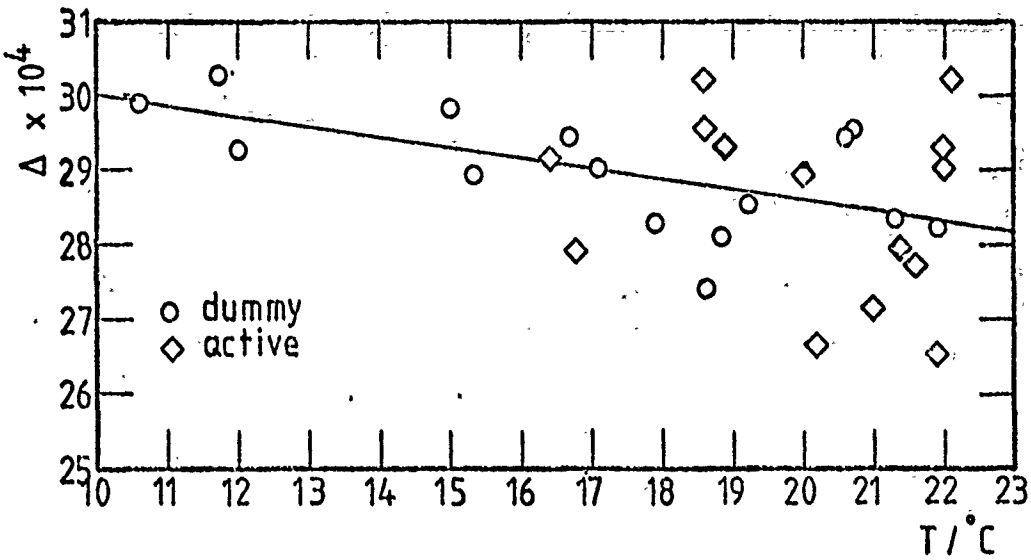

Figure 19. Temperature dependence of logarithmic decrement.

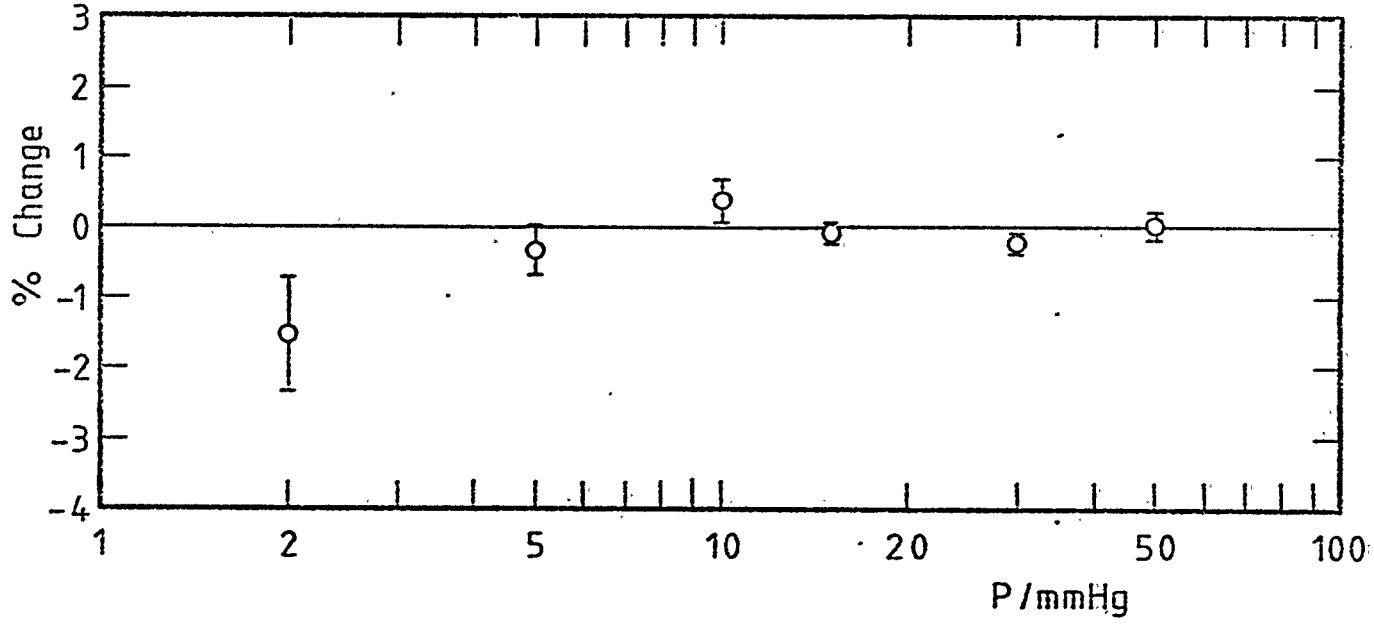

Figure 20. Drag Change on Irradiation (fully turbulent flow).

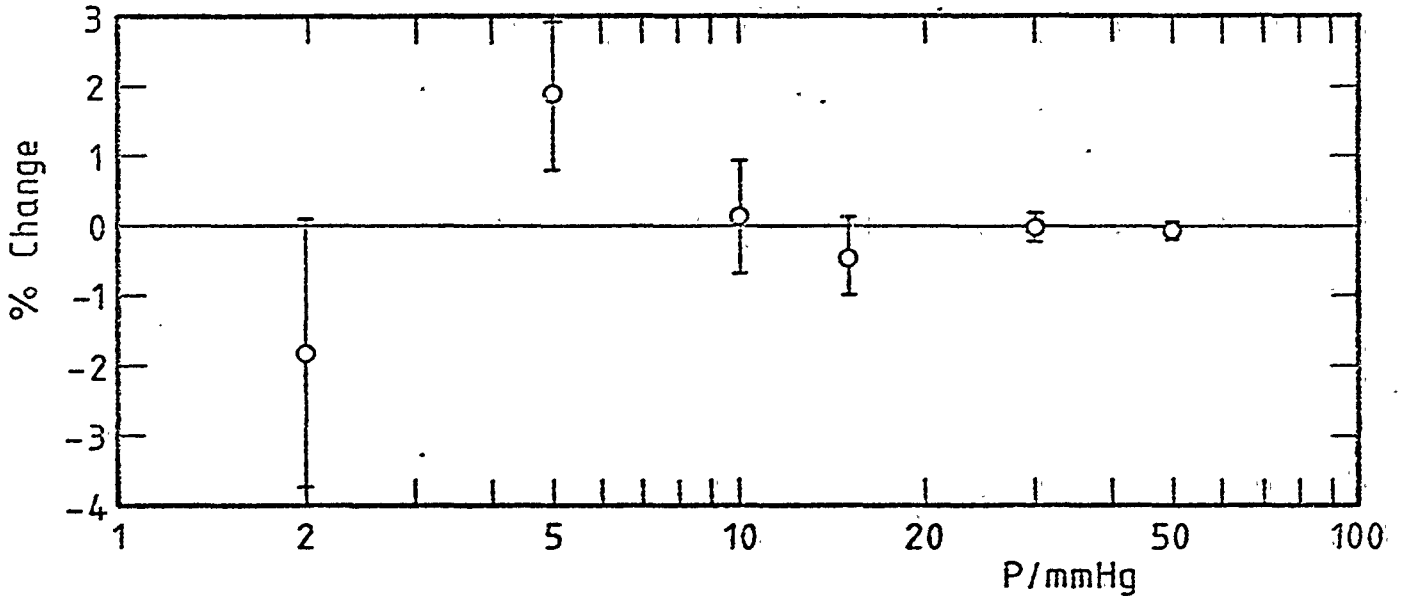

Figure 21. Drag Change on Irradiation

(laminar / transitional flow).

TABLE 1

DRAG MEASUREMENTS IN FULLY TURBULENT FLOW

Expt.	Plate	T /°C	Calib./(gf/mV)	r^2	Drag/mV P = 2	5	10	15	30	50 mmHg
C401										
D402	N2	18.2			3.6	8.3	15.3	22.6	42.6	67.6
C403										
D404	N4	18.8			3.7	8.2	15.1	22.5	42.3	67.6
C405		19.1	0.08842	0.99999						
C406		19.4	0.08929	0.99999						
D407	N5	19.4			3.5	8.1	15.2	22.6	42.8	67.8
C408		19.8	0.08912	0.99999						
D409	N3	19.8			3.6	8.0	15.1	22.7	42.8	67.8
C410		19.6	0.08845	0.99999						
C411		20.0	0.08838	0.99999						
D412	N1	20.1			3.5	8.0	15.1	22.4	42.6	67.7
C413		20.1	0.08871	0.99998						
D414	N2	20.0			3.4	8.0	15.1	22.5	42.6	67.8
C415		20.1	0.08952	0.99999						
C416		20.7	0.08914	0.99999						
D417	N3	20.7			3.6	8.3	15.3	22.7	42.8	68.0
C418		20.6	0.08940	0.99998						
D419	N4	20.4			3.8	8.1	15.0	22.7	42.9	68.2
C420		20.4	0.08883	1.00000						
C421		20.9	0.08897	0.99998						
D422	N5	20.9			3.5	8.0	15.2	22.6	43.1	67.9
C423		20.6	0.08870	1.00000						
D424	N1	21.1			3.6	8.0	15.1	22.7	42.7	67.9
C427		21.2	0.08920	0.99999						
D428	A1	21.0			3.5	8.0	15.3	22.4	42.7	68.1
C429		20.9	0.08942	0.99998						
D430	N2	21.2			3.5	8.0	15.1	22.5	42.6	68.1
C431		21.2	0.08897	0.99999						

TABLE 1 (continued)

C432		21.5	0.08854	0.99999							
D433	N3	21.2			3.5	8.1	15.2	22.4	42.7	68.0	
C434		21.7	0.08942	0.99999							
D435	N4	21.4			3.6	8.0	15.1	22.3	42.8	68.3	
C436		21.8	0.08925	0.99999							
D437	A2	21.5			3.4	8.0	15.3	22.5	42.7	68.4	
C438		21.5	0.08849	0.99997							
D439	N5	21.7			3.6	8.1	15.1	22.4	42.6	68.2	
C440		21.7	0.08843	0.99997							
C501		19.0	0.08959	0.99999							
C502		19.0	0.08886	0.99999							
D503	N3	18.8			3.6	8.1	15.1	22.4	42.3	67.2	
C504		19.1	0.08944	0.99998							
D505	N4	19.1			3.6	8.1	15.0	22.6	42.3	67.5	
C506		20.2	0.08886	0.99994							
D507	A2	19.8			3.6	8.2	15.1	22.5	42.4	67.8	
C508		19.8	0.08918	0.99999							
D509	N5	20.0			3.6	8.1	15.1	22.6	42.5	67.2	
C510		20.0	0.08827	0.99999							
C511		20.9	0.08918	0.99999							
D512	N1	20.5			3.3	8.1	15.2	22.4	42.4	67.4	
C513		21.0	0.08916	0.99998							
D514	A1	20.7			3.6	7.9	15.1	22.6	42.3	67.6	
C515		20.7	0.08902	0.99999							
C516		21.3	0.08936	0.99998							
D517	N2	21.0			3.6	8.0	15.1	22.4	42.7	67.9	
C518		21.0	0.08865	0.99998							
D519	N3	21.3			3.7	8.3	15.0	22.5	42.6	68.0	
C520		21.8	0.08881	0.99999							
D521	N4	21.5			3.6	8.0	15.1	22.4	42.6	67.4	
C522		22.0	0.08895	1.00000							
D523	A2	21.7			3.5	8.0	15.1	22.5	42.7	67.6	
C524		21.7	0.08865	0.99999							

TABLE 1 (continued)

C525		22.2	0.08901	1.00000							
D526	N5	21.9			3.7	8.0	15.2	22.6	42.6	68.1	
C527		22.0	0.08959	0.99999							
D528	N1	22.1			3.6	8.0	15.0	22.4	42.7	67.8	
C529		22.6	0.08891	0.99999							
D530	A1	22.3			3.4	7.9	15.0	22.5	42.7	67.9	
C531		22.4	0.08840	1.00000							
D532	N2	22.4			3.5	8.0	15.1	22.5	42.6	68.0	
C533		22.4	0.08906	1.00000							
C534		22.7	0.08870	1.00000							
D535	N4	22.5			3.5	7.9	15.0	22.2	42.7	67.9	
C536		22.9	0.08939	0.99998							
D537	A2	22.6			3.5	7.9	15.2	22.4	42.6	67.7	
C539		22.3	0.08887	0.99998							
D540	N5	22.7			3.5	7.9	15.1	22.5	42.9	68.1	
C541		22.9	0.08943	0.99999							
D542	N1	22.8			3.6	7.8	14.9	22.4	42.5	67.9	
C543		23.1	0.08871	0.99999							
D544	A1	23.1			3.5	7.9	15.2	22.5	42.6	68.3	
C545		22.9	0.08878	0.99999							
D546	N2	23.0			3.6	7.8	15.0	22.6	42.7	67.8	
C547		23.0	0.08904	0.99999							
C548		23.1	0.09132	0.99901							
D549	N3	22.9			3.6	7.9	15.2	22.7	42.8	67.9*	
C550		23.1	0.08943	0.99999							
D551	N4	22.9			3.3	7.9	15.1	22.4	42.7	67.9	

TABLE 2

DRAG MEASUREMENTS IN LAMINAR AND TRANSITIONAL FLOW

Expt.	Plate	T_h/ °C	Calib./(gf/mV)	r^2	Drag/mV P = 2	5	10	15	30	50 mmHg
C601		16.1	0.08951	0.99999						
C602		16.1	0.09014	0.99997						
C603		16.0	0.08875	0.99999						
C604		16.0	0.08898	0.99997						
D605	N1	16.1			1.3	2.4	6.7	13.3	32.7	53.0
D606	A1	16.9			1.3	2.3	6.7	13.1	32.8	53.1
D607	N2	17.1			1.3	2.5	6.8	13.2	32.7	53.4
D608	N3	17.4			1.3	2.5	6.6	12.9	32.8	53.4
D609	A2	17.8			1.4	2.6	6.7	12.9	32.7	53.3
D610	N4	17.9			1.4	2.5	6.5	12.9	32.6	53.5
C611		17.9	0.08894	0.99999						
C612		17.8	0.08840	0.99997						
C613		17.8	0.08909	0.99999						
C614		17.8	0.08893	0.99998						
D615	N1	18.1			1.5	2.5	6.7	12.9	32.6	53.3
D616	A1	18.1			1.5	2.6	6.7	13.0	32.5	53.3
D617	N2	18.3			1.5	2.5	6.5	13.1	32.5	53.4
D618	N3	18.5			1.4	2.4	6.7	13.0	32.3	53.3
D619	A2	18.6			1.3	2.6	6.6	12.8	32.4	53.4
D620	N4	18.7			1.5	2.5	6.5	13.0	32.3	53.3
C621		18.7	0.08875	0.99994						
C622		18.7	0.08847	0.99999						
C623		18.7	0.08897	0.99999						
C624		18.7	0.08845	0.99999						
D625	N1	18.8			1.3	2.5	6.7	12.7	32.5	53.5
D626	A1	19.0			1.4	2.6	6.4	12.3	32.6	53.5
D627	N2	19.1			1.4*	2.5	6.6	12.5	32.6	53.7
D628	N3	19.2			1.4	2.5	6.8	12.2	32.6	53.4
D629	A2	19.2			1.4	2.6	6.7	12.2	32.5	53.3
D630	N3	19.3			1.5	2.6	6.5	12.1	32.5	53.5

TABLE 2 (continued)

C631		19.3	0.08898	0.99998							
C632		19.2	0.08879	0.99999							
C633		19.2	0.08988	0.99998							
C634		19.2	0.08966	0.99999							
D635	N1	19.2			1.4	2.6	6.3	12.3	32.8	53.7	
D636	A1	19.1			1.3	2.7	6.2	12.2	32.7	53.7	
D637	N2	19.1			1.4	2.4	6.3	12.4	32.7	53.6	
D638	N3	19.1			1.3	2.4	6.3	12.2	32.4	53.7	
D639	A2	19.2			1.3	2.6	6.5	12.4	32.4	53.4	
D640	N4	19.3			1.5	2.4	6.4	12.5	32.5	53.5	
C641		19.3	0.08928	0.99998							
C642		19.3	0.08970	0.99997							
C701		16.0	0.08920	0.99998							
C702		16.0	0.08933	0.99998							
D703	N2	15.9			1.4	2.4	6.7	13.2	32.4	53.1	
D704	A1	16.3			1.4	2.4	6.8	13.4	32.2	53.2	
D705	N2	16.6			1.5	2.4	6.6	13.4	32.5	53.1	
D706	N3	16.8			1.4	2.4	6.7	13.1	32.6	52.9	
D707	A2	17.0			1.4	2.4	6.6	12.9	32.6	52.9	
D708	N4	17.3			1.4	2.4	6.8	13.1	32.9	53.2	
C709		17.3	0.08863	0.99998							
C710		17.4	0.08871	0.99999							
C711		17.4	0.08878	0.99999							
C712		17.4	0.08929	0.99999							
D713	N2	18.0			1.4	2.6	6.8	12.9	32.6	53.3	
D714	A1	18.1			1.5	2.5	6.7	12.7	32.8	53.4	
D715	N2	18.4			1.5	2.6	6.7	12.7	32.9	53.3	
D716	N3	18.5			1.5	2.6	6.7	12.6	32.7	53.1	
D717	A2	18.9			1.4	2.5	6.7	12.8	32.8	53.3	
D718	N4	18.8			1.3	2.5	6.5	12.6	32.3	52.9	
C719		18.8	0.08855	0.99999							
C720		18.8	0.08879	0.99998							
C721		18.7	0.08912	0.99999							
C722		18.7	0.08849	0.99972							

TABLE 3

DRAG VALUES FOR FULLY TURBULENT FLOW

Mean and Standard Error (in mV) quoted. Calibration = 0.0890 ± 0.0002 gf/mV . Corrected to 20°C.

P/mmHg	N		A1		A2		A	
2	3.583	0.019	3.534	0.036	3.527	0.036	3.530	0.023
5	8.104	0.017	8.044	0.035	8.119	0.025	8.081	0.024
10	15.120	0.017	15.173	0.064	15.193	0.052	15.183	0.038
15	22.529	0.025	22.539	0.043	22.506	0.020	22.522	0.022
30	42.598	0.034	42.484	0.083	42.529	0.053	42.507	0.048
50	67.72	0.045	67.78	0.12	67.72	0.20	67.75	0.11

TABLE 4

DRAG VALUES FOR LAMINAR/TRANSITIONAL FLOW

Values in mV, corrected to 20°C. Calibration = 0.08905 ± 0.00009 gf/mV .

P/mmHg	N		A1		A2		A	
2	1.420	0.016	1.414	0.037	1.377	0.022	1.395	0.021
5	2.575	0.015	2.619	0.042	2.626	0.026	2.623	0.023
10	6.449	0.029	6.413	0.067	6.507	0.043	6.460	0.041
15	12.203	0.040	12.131	0.072	12.181	0.084	12.156	0.053
30	32.570	0.038	32.585	0.094	32.555	0.065	32.570	0.057
50	53.613	0.040	53.676	0.040	53.497	0.053	53.586	0.049

TABLE 5

% DRAG CHANGES ON IRRADIATION (FULLY TURBULENT FLOW)

(maximum accuracy quoted :- nearest 0.05)

P/mmHg	A1	A2	A
2	-1.4 ± 1.1	-1.6 ± 1.1	-1.5 ± 0.8
5	-0.75 ± 0.5	+0.2 ± 0.35	-0.3 ± 0.35
10	+0.35 ± 0.45	+0.5 ± 0.35	+0.4 ± 0.3
15	+0.05 ± 0.2	-0.1 ± 0.15	-0.05 ± 0.15
30	-0.25 ± 0.2	-0.15 ± 0.15	-0.2 ± 0.15
50	+0.1 ± 0.2	0.0 ± 0.3	+0.05 ± 0.2

TABLE 6

% DRAG CHANGES ON IRRADIATION (LAMINAR/TRANSITIONAL FLOW)

(maximum accuracy quoted :- nearest 0.05)

P/mmHg	A1	A2	A
2	-0.4 ± 2.8	-3.0 ± 1.9	-1.8 ± 1.9
5	+1.7 ± 1.7	+2.0 ± 1.2	+1.9 ± 1.1
10	-0.6 ± 1.1	+0.9 ± 0.8	+0.15 ± 0.8
15	-0.6 ± 0.65	-0.2 ± 0.75	-0.4 ± 0.55
30	+0.05 ± 0.3	-0.05 ± 0.25	0.0 ± 0.2
50	+0.1 ± 0.1	-0.2 ± 0.1	-0.05 ± 0.1

TABLE 7

Preliminary experiments

wire	dia/mm	Δ
steel(piano)	0.127	0.0088 ; 0.0058
98Cu/2Be	0.051	0.030
"	0.149	0.048 $\pm$ 0.0006

TABLE 8

Experiments with ^{147}Pm

	$\Delta \times 10^6$	
Base prized off between experiments		
dummy	4999 $\pm$ 9	
active	5053 $\pm$ 11	$\frac{\delta\Delta}{\Delta}$ =0.995 $\pm$ 0.003
dummy	5156 $\pm$ 9	
Base removed;viscometer propped		
dummy	4693 $\pm$ 17	
active	4824 $\pm$ 35	$\frac{\delta\Delta}{\Delta}$ =1.030 $\pm$ 0.008
dummy	4676 $\pm$ 17	
dummy	5078 $\pm$ 63	
active	5130 $\pm$ 31	$\frac{\delta\Delta}{\Delta}$ =0.995 $\pm$ 0.010
dummy	5229 $\pm$ 49	
Base prized off between experiments;heavy disc		
dummy	2866 $\pm$ 23	
active	2920 $\pm$ 18	$\frac{\delta\Delta}{\Delta}$ =1.016 $\pm$ 0.008
dummy	2884 $\pm$ 22	

Combined result: Change in viscosity on irradiation from ^{147}Pm is

$+(0.08 \pm 0.26)\%$

TABLE 9

Sensitivity to misreading

z = centre of oscillation on scale , cm .

l = distance from viscometer to scale , cm .

z	l	$\Delta \times 10^6$
39.0	237	2500
39.1	237	2616
39.9	237	2716
40.0	237	2742
41.0	237	3025
40.0	232	2742
40.0	242	2742

l accurate to $\pm$ 5 cm $\Rightarrow$ Δ accurate to $< 0.05\%$

z accurate to $\pm$ 1 mm $\Rightarrow$ Δ accurate to ~ 1 %

z accurate to $\pm$ 1 cm $\Rightarrow$ Δ accurate to ~ 9 %

TABLE 10

^{58}Co source

Expt code	$\Delta \times 10^6$	T°C	
D00	3030	11.7	dummy
D11	2991	10.6	dummy
D12	2931	12.0	dummy
D13	2986	15.0	dummy
D14	2947	16.7	dummy
D15	2857	19.2	dummy
D16	2956	20.7	dummy
D21	2665	20.2	active
D22	2877	20.5	active
D23	2716	21.0	active
D24	2772	21.6	active
D25	2934	22.0	active
D26	2904	22.0	active
D27	2656	21.9	active
D31	2831	17.9	dummy
D32	2742	18.6	dummy
D33	2812	18.8	dummy
D34	2945	20.6	dummy
D41	2959	18.6	active
D42	3025	18.6	active
D43	2796	16.8	active
D44	2920	16.4	active
D61	2897	15.3	dummy
D62	2907	17.1	dummy
D63	2826	21.9	dummy
D64	2837	21.3	dummy
D71	2932	18.9	active
D72	2897	20.0	active
D73	2796	21.4	active
D74	3023	22.1	active

$\Delta = 2900 \pm 21$ dummy
$\Delta = 2858 \pm 31$ active
} uncorrected for temperature

Regression of Δ on T :

$\Delta = 3141 - 14.0\ T$

$r^2 = 0.37$

values of Δ corrected to 20°C :

$\Delta = 2860 \pm 16$ dummy

$\Delta = 2860 \pm 30$ active

Change of viscosity on irradiation from ^{58}Co is :

$(0.0 \pm 1.2)\%$